Post-depositional effects on the microstructure and stable isotopes composition of planktic foraminiferal tests from the Miocene of the Pelotas Basin, south Brazilian continental margin

Geise de Santana dos Anjos-Zerfass[1,*], Farid Chemale Jr.[2], and Candido A. V. Moura[3]

[1] BPA/PDEXP/CENPES/PETROBRAS, Av. Horácio Macedo, 950, prédio 20, 1120, 21941-915, Cidade Universitária, Ilha do Fundão, Rio de Janeiro, RJ, Brazil.
[2] Laboratório de Geologia isotópica da Universidade Federal do Rio Grande do Sul, Av. Bento Gonçalves, 9500, Porto Alegre, 91501-970, Brazil.
[3] Universidade Federal do Pará, Centro de Geociências, Departamento de Geoquímica e Petrologia. Rua Augusto Corrêa nº 1, Guamá, 66075-900 - Belém, 8608, Brazil.
**geise.zerfass@petrobras.com.br*

ABSTRACT

An integrated study of planktic foraminiferal tests (Orbulina universa and Globigerinoides trilobus) imaging techniques and chemical/isotopic analyses has been carried out at the Miocene section of the Pelotas Basin (South Brazil) with the purpose of record and evaluate the effects of the diagenesis in its wall texture and isotopic composition. The characterization of the foraminiferal tests preservation prior performing isotopic analysis for paleoceanographic studies is essential to ensure the choice of suitable material for obtaining reliable data. Scanning electron microscopy, backscatter scanning electron microscopy, energy-dispersive X-ray spectrometry and stable isotope measurements were used to evaluate the post-depositional effects on the tests. It was possible to identify features of dissolution, neomorphism (recrystallization) and coating of autigenic minerals. The stable isotopic data define two compositional groups. The heavier and less scattered values characterize a preserved paleoenvironmental signal as the lighter and scattered ones indicate a signal derived from post-depositional alterations. Additionally, the characterization of the distinct types of diagenetic changes and their textural products provide a guideline for the evaluation of the diagenetic effects of deeply buried fossil foraminifera.

Key words: planktic foraminifera tests, diagenesis, stable isotopes, Miocene, Pelotas Basin, Brazil.

RESUMEN

Un estudio integrado de las características de textura y composición química e isotópica de foraminíferos planctónicos (Orbulina universa y Globigerinoides trilobus) del Mioceno de la Cuenca de Pelotas (sur de Brasil) fue llevado a cabo con el propósito de registrar y evaluar los efectos de la diagénesis. La caracterización del grado de preservación de los foraminíferos, previa a la obtención de análisis isotópicos para estudios paleoceanográficos, es esencial para asegurar una selección adecuada del material y así obtener datos fiables. Se empleó microscopía electrónica de barrido, imágenes con

dos Anjos-Zerfass G.S., Chemale, F. Jr., Moura, C.A.V. 2011, Post-depositional effects on the microstructure and stable isotopes composition of planktic foraminiferal tests from the Miocene of the Pelotas Basin, south Brazilian continental margin: Revista Mexicana de Ciencias Geológicas, v. 28, núm. 1, p. 92-104.

electrones retrodispersados, espectroscopía de rayos X de dispersión de energía y mediciones de isótopos estables para evaluar los efectos post-depósito en los caparazones. Esos estudios permitieron identificar características de disolución, recristalización y revestimiento de minerales autigénicos. Los datos de isótopos estables permitieron definir dos grupos de composición: los valores más pesados y menos dispersos caracterizan señales paleoambientales preservadas, mientras que los datos más dispersos y correspondientes a composiciones más ligeras indican una señal derivada de las alteraciones post-depósito. Además, la caracterización de los distintos tipos de cambios diagenéticos y sus productos texturales proporciona una guía para la evaluación de los efectos diagenéticos en los foraminíferos fósiles provenientes de secciones sedimentarias de gran espesor.

Palabras clave: foraminíferos planctónicos, diagénesis, isótopos estables, Mioceno, Cuenca de Pelotas, Brasil.

INTRODUCTION

The chemical and isotopic compositions of planktic foraminifera tests are widely used as paleoclimatic and paleoceanographic proxies. However, the susceptibility of foraminiferal tests to post-depositional processes, such as dissolution and precipitation of secondary phases, makes difficult to interpret the paleoenvironmental data (Lohmann, 1995; Brown and Elderfield, 1996; Shieh *et al.*, 2002; Sadekov *et al.*, 2010).

The more significant alterations caused by diagenesis in the marine organism tests are dissolution and neomorphism of aragonite to calcite, which cause changes in the trace element composition such as strontium and magnesium removal (Faure, 1986). Diagenesis acts to alter the paleoceanographic signal of the foraminifera calcite test, since the precipitation of secondary calcite and the dissolution of the tests tend to shift the oxygen isotopic composition towards a negative direction, resulting in warmer $\delta^{18}O$-derived paleotemperatures (Savin and Douglas, 1973; Killingley, 1983; Williams *et al.*, 2005). The addition of secondary calcite presents a high potential of changing the Mg/Ca ratio, while the inorganic calcite has a higher proportion of magnesium than the biogenic calcite, causing erroneous paleotemperature estimates (Sexton *et al.*, 2006).

The presence of overgrowths and/or neomorphic calcite on the micrometric scale is sometimes impossible to detect under binocular microscope (Sexton *et al.*, 2006; Williams *et al.*, 2007). Consequently, the foraminifera tests presenting this class of alteration preserve the microstructural features and, as a result, are frequently assumed to be well preserved. However, scanning electron microscopy constitutes an efficient method for appraising the diagenetic effects in materials presenting a systematic structure such as the biogenic carbonates, for which the good preservation of the morphological characteristics indicates sample integrity (McArthur, 1994). This technique is widely used in the evaluation of fossil foraminifera preservation (Adelseck, 1978; Sexton *et al.*, 2006, Williams *et al.*, 2007).

This paper presents an evaluation of the post-depositional effects on the wall texture and isotopic composition of two common species of planktic foraminifera, *Globigerinoides trilobus* and *Orbulina universa*, using scanning electron microscopy - SEM, stable isotope evaluation and energy dispersive X-ray spectrometry - EDS data and represents a case study on the effects of diagenesis in foraminiferal tests under great burial depths. Furthermore, we present an image guide to the differences between the various states of preservation.

GEOLOGICAL SETTING

The Pelotas Basin corresponds to the portion of the South American continental margin between 28º40'S and 34ºS, limited to the north by the Florianópolis High, Brazil, and to the south by the Polonio High, Uruguay (Kowsmann *et al.*, 1974; Rosa, 2007). The basin has an area of about 210,000 km^2, from which about 40,000 km^2 occurs as emerged area (Figure 1).

The chronostratigraphic interval focused on in this paper corresponds to the Miocene, according to the relative dating using the $^{87}Sr/^{86}Sr$ ratio presented by Chemale Jr. *et al.* (2002) and Anjos-Zerfass (2009). In terms of the litostratigraphic framework, this interval is positioned in the context of Cidreira and Imbé formations that constitute the regressive depositional sequence of the basin (Bueno *et al.* 2007). The Cidreira Formation consists of clastics deposited in transitional environmental settings with ages ranging from Turonian to Holocene, while the Imbé Formation corresponds to shales with intercalated turbiditic sandstones with ages ranging from Turonian to Recent (Dias *et al.* 1994).

MATERIAL AND METHODS

A total of 66 samples were collected from five wells drilled in the Pelotas Basin, southernmost Brazil, four of which in the offshore segment of the basin and one in the onshore portion (Figure 1). Samples from drill-holes PEL-1, PEL-2, and PEL-3 are cutting, whereas those from 2-TG-96-RS and PEL-2A are from cores. Scanning electron microscopy analyses were carried out on foraminiferal tests from 57 samples, and isotopic analyses were performed in the tests recovered from 46 samples (Figure 2).

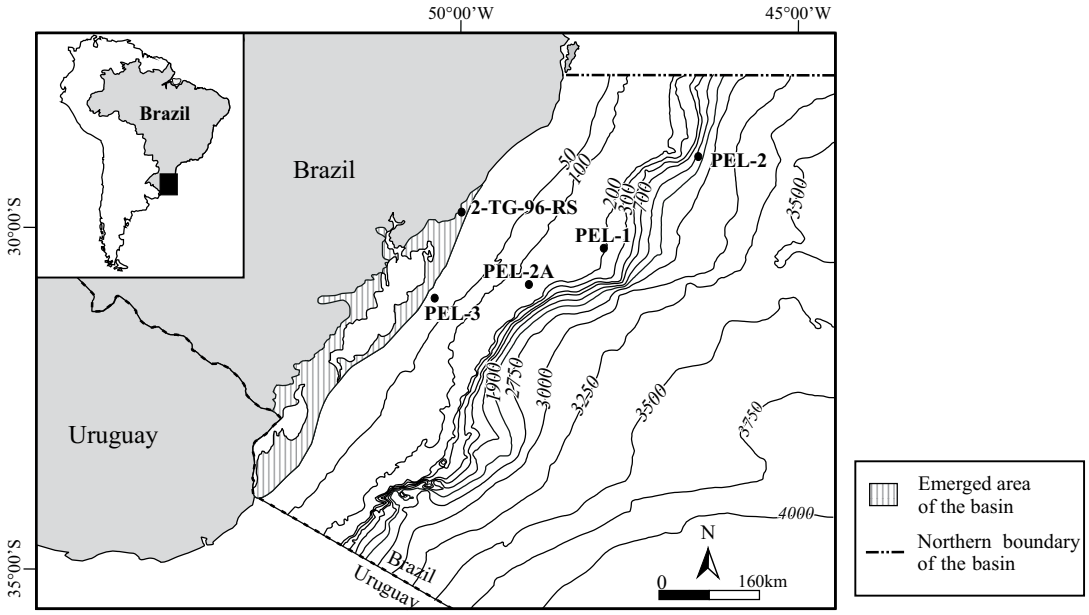

Figure 1. Location map for the Brazilian portion of the Pelotas Basin with the situation of the studied drill-holes.

The samples were prepared following the conventional techniques for calcareous microfossils. Planktonic specimens from the >150 μm sieve fraction were hand-picked under a stereomicroscope Olympus-SZ1145. Well-preserved specimens were separated for isotopic analyses and then ultrasonically cleaned with ultrapure (Milli-Q) water in order to remove particles adhered to the tests.

Analyses by energy dispersive X-ray spectrometry (EDS), backscattered electron microscopy (BSEM) and scanning electron microscopy (SEM) imaging were carried out at the Electron Microscopy Center of the UFRGS with a JEOL JSM 5800 (BSEM and EDS) and JEOL JSM 6060 (SEM) microscopes with a power output of 10kV. Specimens intended for analysis were coated with an alloy of gold and palladium.

EDS mapping was performed in specimens presenting oxidized coatings in order to characterize the chemical composition and superficial distribution of the contaminant phases. SEM imaging was used to document the microstructural features of specimens of *Globigerinoides trilobus* and *Orbulina universa*. These were chosen for the microstructural analyses because they are widely used in paleoenvironmental and paleoceanographic reconstructions (*e.g.* Spero and Lea, 1993; Bemis *et al.*, 1998, 2000; Sanyal *et al.*, 2001; Zeebee *et al.*, 2008) and also because they are abundant in the samples studied.

Carbon and oxygen isotope analyses were carried out in 54 monogeneric samples, of which 26 are from drill-hole PEL-1, 26 from drill-hole PEL-2 and two from the well PEL-2A. Isotopic analyses were performed at the Isotope Geology Laboratory of the Federal University of Pará, Brazil (Para-Iso). CO_2 gas was extracted from the foraminiferal tests (1 – 6 individuals) with 100% orthophosphoric acid at

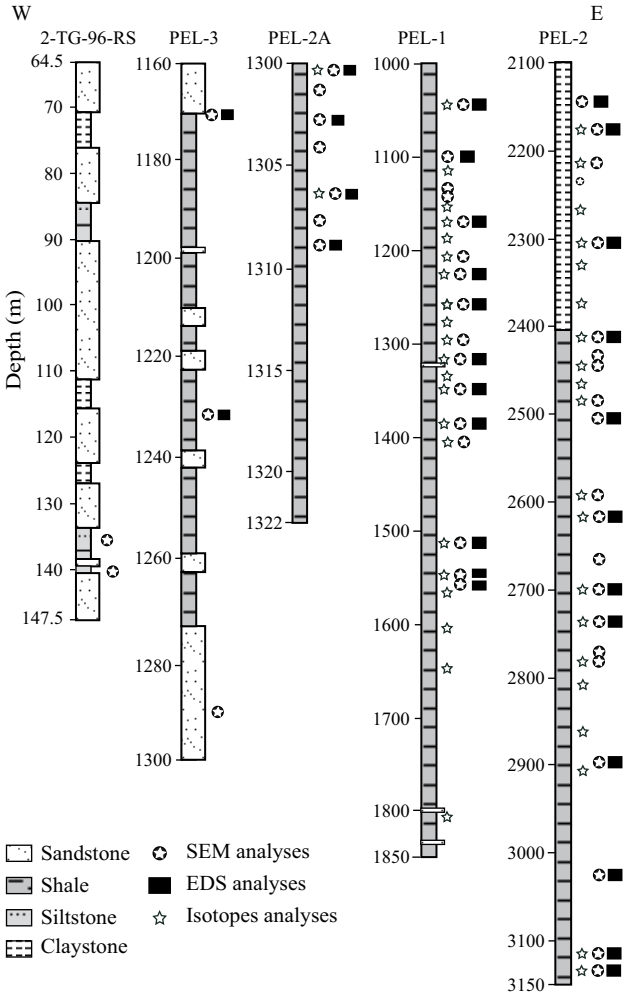

Figure 2. Columnar section of the studied intervals of the selected drill-holes, showing the position of the analyzed samples.

70°C, using an on-line KIEL-III system coupled to the mass spectrometer Finnigan MAT 252. The results are reported in the conventional δ notation as per mil (‰) relative to the Chicago PDB standard. The analysis of the standard NBS-19, during the course of this study, has yield average $\delta^{13}C$ and $\delta^{18}O$ values of 2.0 ‰ and -2.13 ‰, respectively. The uncertainties of the isotope measurements are better than 0.07 % for carbon and 0.14 % for oxygen, based on replicated analysis of the NBS-19 carbonate standard.

The terminology used in this study follows nomenclature proposed by Sexton *et al.* (2006) to describe processes involving the addition of inorganic calcite to the foraminiferal calcite. The term "neomorphism" was used instead of "recrystallization," whereas "calcite infill" was assigned to the growth of inorganic calcite crystals of micrometric scale that complete chamber filling.

RESULTS AND DISCUSSION

Scanning electron microscopy

The differentiation between distinct types of diagenetic changes is essential for the recognition of the processes that cause obliteration of the microfossiliferous record. In this context, the evaluation of microstructure preservation promotes the study of the nature of post-depositional processes. Indeed, is important to define the characteristic patterns of a species before being able to recognize the alterations caused by diagenesis.

In terms of microstructural characteristics, *Orbulina universa* presents pore-like apertures scattered across the surface of the last chamber surface, which is densely perforated and commonly presents pores of two different sizes (Bolli and Saunders, 1985; Kennett and Srinivasan, 1983). As opposed to some authors who consider the bilobate forms of *Orbulina* as a separate species (*Orbulina bilobata*), we follow the taxonomic descriptions of Stainforth *et al.* (1975) and Bolli and Saunders (1985), both of whom consider these forms as a variation of *Orbulina universa*.

Globigerinoides trilobus subspecies are distinguished only by the morphology of the final chamber, which is larger then the other chambers combined in the subspecies *trilobus*, is slightly smaller when compared with *trilobus* in the subspecies *immaturus* and is sac-like in the subspecies *sacculifer* (Bolli and Saunders, 1985). On the other hand, considering the microstructural features of the wall, the three subspecies are identical. The microstructure of *Globigerinoides trilobus* corresponds to a densely perforated wall with a cancellate pattern and pores situated in well-developed pore pits separated by interpore elevations (Kennet and Srinivasan, 1983).

Signals of mechanical alterations were observed in specimens of both studied genera. The removal of parts of the outer surface of the test was observed mostly in *Globigerinoides* specimens, while breakage was more commonly observed in *Orbulina* specimens. Peeling can be an artifact of the sample preparation, and it acts to obliterate the original wall texture of the test by means of exposing the internal layers that present attenuated topography (Sexton *et al.*, 2006). Breakage occurs due to the fragility of the tests under mechanical abrasion or as a consequence of the calcite infilling.

Three types of chemical alteration were observed in the tests collected at different levels of the studied drill-holes: (1) oxidized coating and/or pyrite infilling; (2) dissolution; and (3) calcite infilling / neomorphism of the biogenic calcite to an inorganic one.

Well-preserved specimens especially occurred between 1,044 and 1,314 m in drill-hole PEL-1 and between 2,142 and 2,448 m in drill-hole PEL-2. In the samples of the other studied wells, conversely, the occurrence of well-preserved tests was rare, as most of the specimens presented visible diagenetic alterations under stereomicroscopy.

The tests exhibiting oxidized coatings commonly occurred in association with well-preserved specimens and were observed only at levels higher than 1,548 m of well PEL-1 and along drill-hole PEL-2. These tests are characterized by spots of orange color, sometimes coating the whole wall texture. The textural features were usually well-preserved but often presented aspects of oxidized films or crusts that obstructed pores and, occasionally, completely obliterated the wall texture (Figure 3). Pyrite occurred as infillings and granules disseminated over and in the tests, generally in specimens that presented oxidized spots that were taken from the intervals between 1,224 and 1,314 m in drill-hole PEL-1 and between 2,664 and 2,700 m in drill-hole PEL-2 (Figure 3).

With the increase of burial depth, the tests presented a rising degree of pervasive neomorphism and calcite infill, with overgrowths of calcite and obliteration of pores and apertures due to secondary carbonate precipitation. Tests presenting a reduction of pore sizes and calcite infilling and/or overgrowths were also observed in depths below 1,332 m in well PEL-1 and below 2,502 m in drill-hole PEL-2. SEM images revealed textural alterations in the wall texture of tests presenting neomorphism features, with increases in crystal size, given the aspect of a mosaic of crystals, as previous observed by Budd and Hiatt (1993) in benthic specimen tests. Figures 4 and 5 illustrate specimens presenting features of calcite infill and neomorphism with pore obstruction, secondary calcite infilling and complete obliteration of the wall texture.

The above-mentioned alteration features are strongly related to the chemical/isotopic changes; therefore, they are better discussed in association with the energy dispersive spectrometry and stable isotope data.

The initial stage of dissolution is characterized by relief degradation and slight enlargement of the pores. In a more advanced stage of dissolution presents fissures in the funnel walls, significant enlargement of the pores and flat-

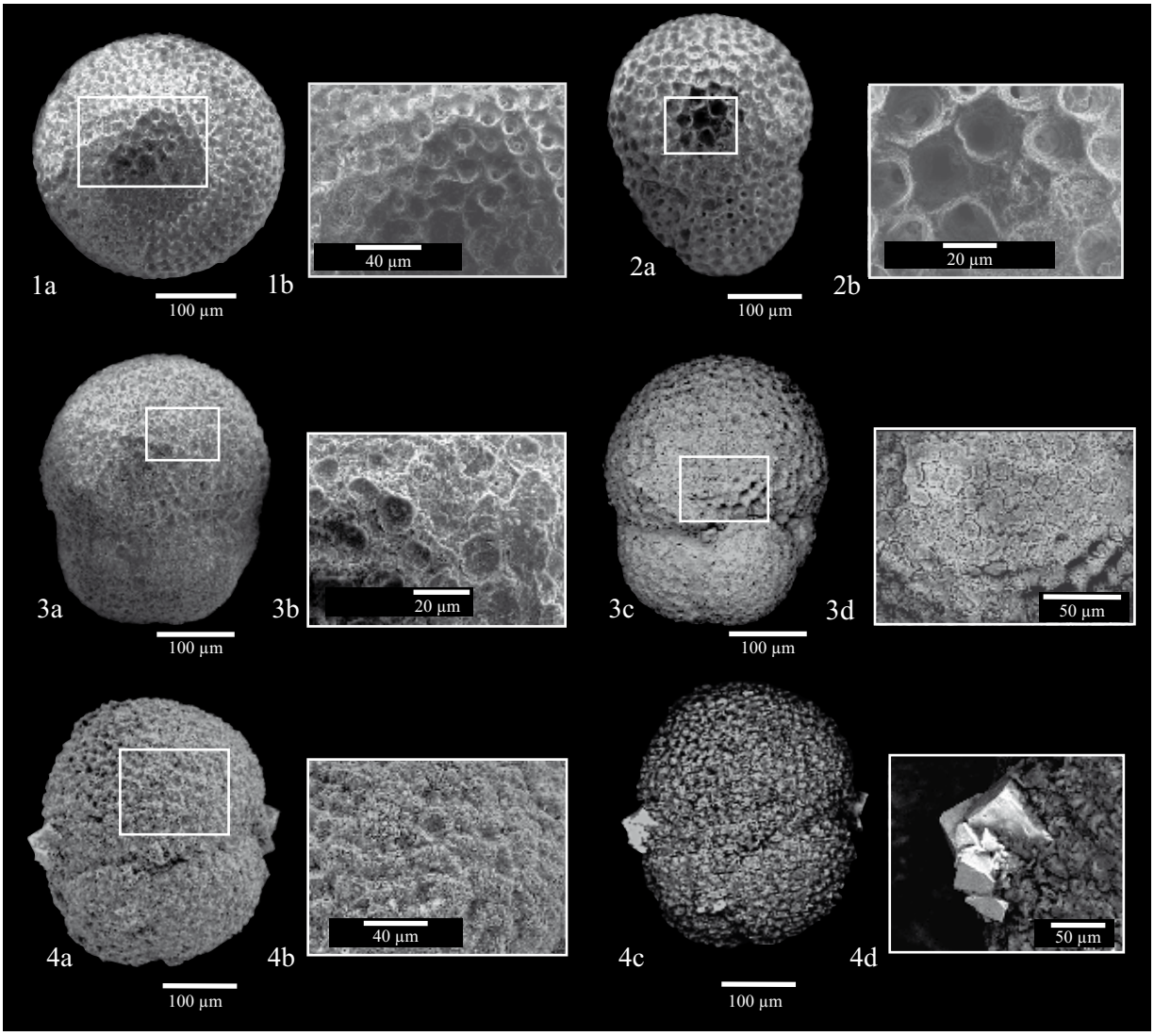

Figure 3. 1a. *Orbulina universa* with oxidized coatings, umbilical view, drill-hole 1 (1,224 m), 1b. Detail showing pores with partial infilling. 2a. *Globigerinoides trilobus* presenting oxidized spots, spiral view, PEL-1 (1,350 m); 2b. Detail showing pores filled by oxide. 3a. *Globigerinoides trilobus* with oxidized crust, umbilical view, drill-hole PEL-3 (1,300 m), 3b. Detail of the wall without textural features; 3c. Backscattering image; 3d. Detail. 4a. *Globigerinoides trilobus* covered with an oxidized crust and with pyrite overgrowths, umbilical view, PEL-2 (2,898 m), 4b. Detail showing oxide crust aspect; 4c. Backscattering image; 4d. Backscattering detail of a pyrite crystal.

tened interpore areas predominantly near the sutures. The most advanced stage is characterized by areas presenting coalescence of pores due to destruction of the interpore areas and fissures through the remaining interpore areas.

Foraminifera tests exhibiting features of dissolution were observed in the samples in the well 2-TG-96-RS, at the higher levels of drill-hole PEL-1 (above 1,224 m) and in a few samples from the drill-holes PEL-3 and PEL-2A samples. Samples from the 2-TG-96-RS well presented indications of pervasive dissolution, whereas the dissolution features were moderate to subtle in the samples of the PEL-1 drill-hole. Specimens of *Globigerinoides trilobus* and *Orbulina universa* from the 2-TG-96-RS and PEL-3 drill-holes were significantly affected by dissolution (Figure 6). In the samples of drill-hole PEL-1, the dissolution features are less important and are represented by small fissures at the pore pit walls, while the dissolution features in drill-hole PEL-2 were not verified.

According to Collen and Burgess (1979), dissolution begins with the removal of the external layers of the test by the smoothing of the surface and, subsequently, the accentuation and widening of the sutural pores. This process is strongly related to the distribution of the pores, which constitute weak points. Consequently, finely perforated species such as *Orbulina universa* and *Globigerinoides trilobus* are intensely affected by dissolution.

Dissolution constitutes one of the most important post-depositional processes affecting the planktic foraminifera. According to Williams *et al.* (2007), the dissolution of the tests can provide the carbonate for the precipitation of

diagenetic calcite. During diagenesis, the primary calcite is dissolved, and it is substituted by secondary calcite precipitates in isotopic equilibrium with the pore fluids (Schrag *et al.*, 1995). The dissolution of foraminifera tests occurs due to the interaction of the tests with the pore waters sub-saturated in calcium carbonate, as secondary calcite precipitation is supplied by pore water ions (Collen and Burgess 1979).

The morphology of the test also influences the resistance to the dissolution, since the species with more densely perforated walls and larger pores are more susceptible than the compact tests with thick walls (Hecht *et al.*, 1975; Stainforth *et al.*, 1975). *Orbulina universa* and *Globigerinoides trilobus* are included among the planktic foraminifera most affected by dissolution.

The occurrence of tests presenting dissolution features was observed in the most proximal wells (onshore, 2-TG-96-RS; shallow platform, PEL-3, PEL-2A and PEL-1). Furthermore, the mentioned alteration occurs in the shallower depths of the wells. In this position of the basin, it is reasonable to assume that the dissolution processes on the carbonate bioclasts may be driving meteoric water infiltration. According to Morad *et al.* (2000), widespread areas of the platform can be exposed by regressive events, and, as

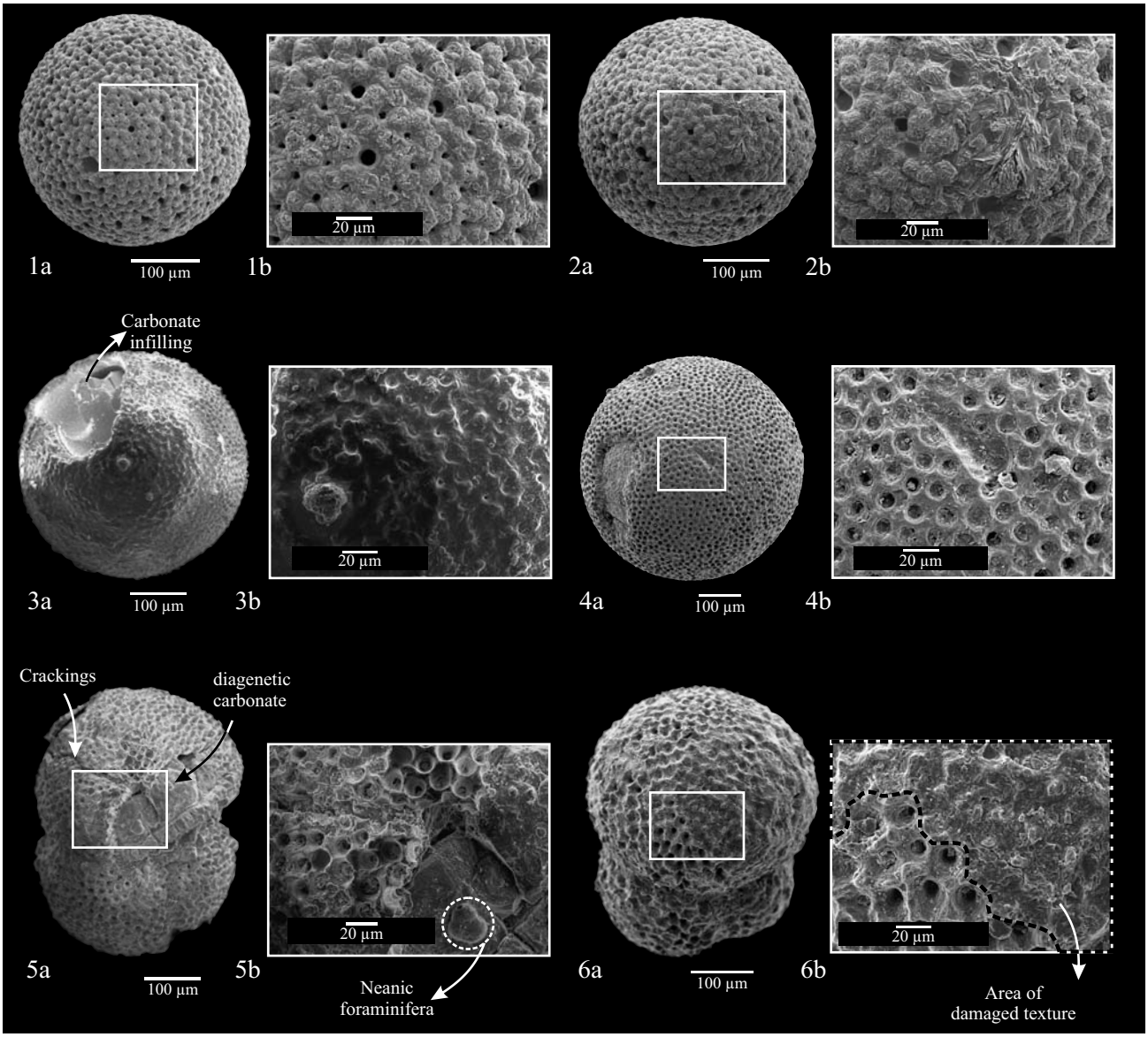

Figure 4. 1a. *Orbulina universa* with slight calcite infilling, PEL-2 (2,232 m); 1b. Detail. 2a. O. universa showing a high degree of calcite infilling. 2b. Detail showing small crystals of calcite; PEL-1 (1,170 m). 3a. *O. universa* with inorganic calcite infilling; 3b. Detail of the wall, with pervasive calcite infilling; PEL-2 (3,132 m). 4a. *O. universa* with calcite infilling; 4b. Detail of the wall showing obstructed pores; drill-hole PEL-3 (1,170 m). 5a. *Globigerinoides trilobus* calcite infilling causing volume increase and rupture of the test, umbilical view, PEL-2 (1,566 m); 5b. detail of the wall showing pervasive calcite infilling; 6a. *G. trilobus* with pervasive calcite infilling, spiral view, drill-hole PEL-2 (1,306.55 m); 6b. Detail of the wall, showing local loss of the textural characters.

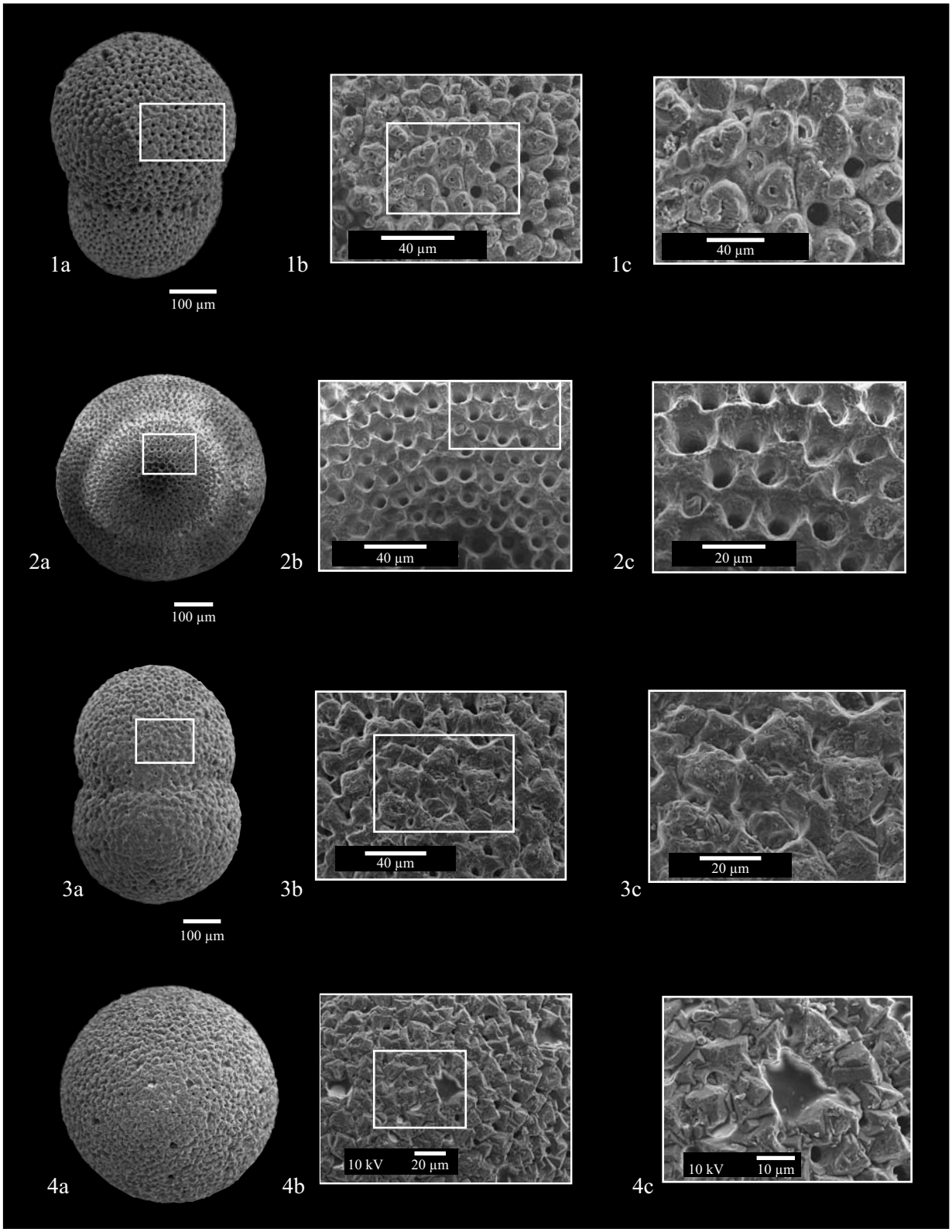

Figure 5. 1a. *Orbulina universa* (bilobate form) with well preserved morphology, PEL-2 (3,024 m); 1b. Detail showing the micro-textural characters; 1c. Detail showing pores and interpore ridges; 2a. Well preserved test of *Orbulina universa*; 2b. Wall texture; 2c. Detail of the wall showing pore pits and interpore areas; 3a. *Orbulina universa* (bilobate form) with wall altered by neomorphism, PEL-2 (2,628 m); 3b. Detail showing obliteration of micro-textural characters; 3c. Detail presenting pore reduction and complete alteration of the interpore area morphology. 4a. *Orbulina universa* test showing altered wall texture, PEL-2 (2,628 m); 4b. Altered wall texture; 4c. Detail showing angular pores and interpore areas composed of large crystals.

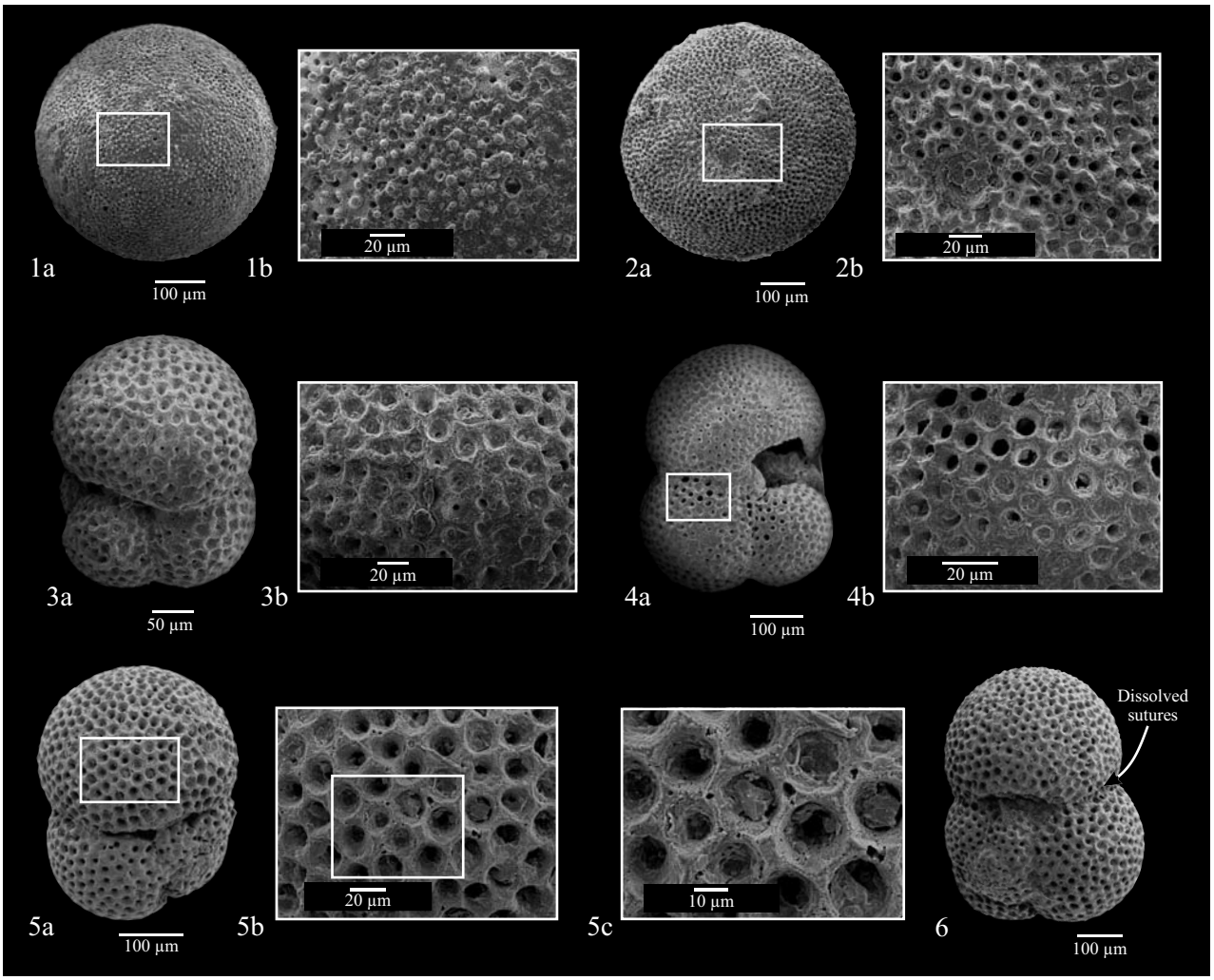

Figure 6. 1a. *Orbulina universa* with dissolution features, PEL-3 (1,230m); 1b. Detail showing dissolution of the surface layer of the wall and local dissolution of the interpore ridges; 2a. *Orbulina universa* with dissolution, PEL-1 (1,566 m); 2b. Detail showing the wall with the removal of greater part of the interpores ridges. 3a. *Globigerinoides trilobus*, 2-TG-96-RS (140.2 m); 3b. Detail showing dissolution of the interpore areas; 4a. *Globigerinoides trilobus* sacculifer with pervasive dissolution, umbilical view, drill-hole 2-TG-96-RS (140.2 m); 4b. Area with complete destruction the pore funnels, drill-hole. 5a. *Globigerinoides trilobus* with extreme dissolution features in the wall, spiral view, drill-hole 2-TG-96-RS (140.2 m). 5b. Detail showing openings in the interpore elevations; 5c. Detail showing pitting through interpore areas and fissures in the pore funnels wall. 6. *Globigerinoides trilobus* immaturus with deepened sutures, and enlarged aperture, spiral view, PEL-1 (1,296 m).

a result, there might be increases in the recharge zones and consequently in the input of meteoric water.

Dissolution could take place during the early diagenetic stage, as there was verified to be an important regressive event in the middle and late Miocene (Dias *et al.*, 1994). Alternatively, this type of alteration could be produced during telodiagenesis. More recent regressive events reported to the early/late Pliocene (Dias *et al.*, 1994) corroborate this assumption.

In diagenetic environments with variable conditions, complex sequences of events can occur. In this way, foraminifera tests can present signals of different diagenetic processes, as with the dissolution followed for calcite crystal overgrowth as previous observed by Collen and Burgess (1979).

Energy dispersive spectrometry

Energy dispersive spectrometry analyses were carried out in specimens collected from 28 samples, of which 11 samples were from drill-hole PEL-1, 11 samples were from drill-hole PEL-2, four samples were from well PEL-2A and two samples were from PEL-3. Punctual analyses carried out in tests with visible signals of neomorphism in SEM had shown that their chemical compositions did not suffer alterations, at least for the levels of major elements (Figure 7).

Specimens exhibiting the oxidized coating and granular pyrite infilling and/or overgrowths were submitted to EDS mapping, revealing compositions with a high percentage of silica and subordinated aluminum, potassium

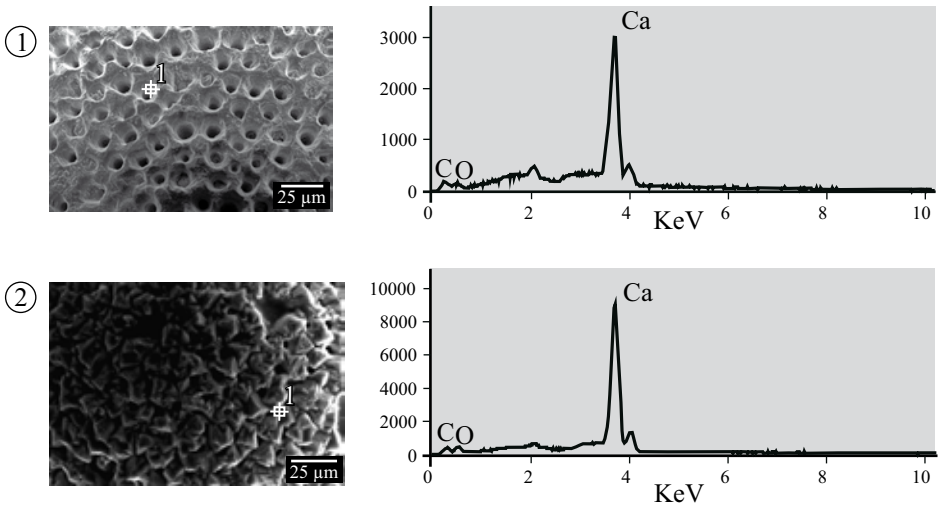

Figure 7. Punctual EDS analyses of *Orbulina universa* specimens. 1. Detail of a well preserved test showing and a punctual chemical composition. 2. Detail of the wall of a test altered by neomorphism, showing unaltered composition.

and magnesium, similar to the composition of clay minerals. EDS maps documented the distribution of calcium, magnesium, aluminum, potassium, silica, iron and sulfur on the surfaces of specimens with oxidized coatings. In Figures 8 and 9, we can observe elemental distribution on the foraminifera test surface, with calcium restricted to the interpore areas while the other elements (Mg, Al, K, Si, Fe and S) appear to be concentrated in the pores.

Based on the compositions and habits of the contaminant phases, we can assume that they correspond to autigenic pyrite and the oxidized coating of glauconite. Autigenic pyrite is formed during sediment burial by the iron mineral reaction with H_2S, which is produced from the reduction of the SO_4 dissolved in the seawater due to the action of anaerobic bacteria (Berner 1981, 1984). Sulfides derived from iron minerals are transformed into pyrite during eodiagenesis by the addition of elemental sulfur originating from bacterial activity (Berner 1981, 1984; Siesser and Roger, 2006). As a result, pyrite formation is also controlled by the amount of detritic iron minerals, which, in the studied sedimentary succession, are composed almost exclusively of the shales that are represented by clay minerals.

According to Odin and Fullagar (1988), glauconite also occurs as coatings covering carbonate bioclasts. Moreover, Closs (1970) reported the occurrence of glauconitized foraminifera associated with glauconitic pellets in the Miocene deposits of the basin. Subsequently, based on the composition, we can presume that the clay mineral coatings observed in the studied samples may be the result of the oxidation of the glauconitic films that cover the tests.

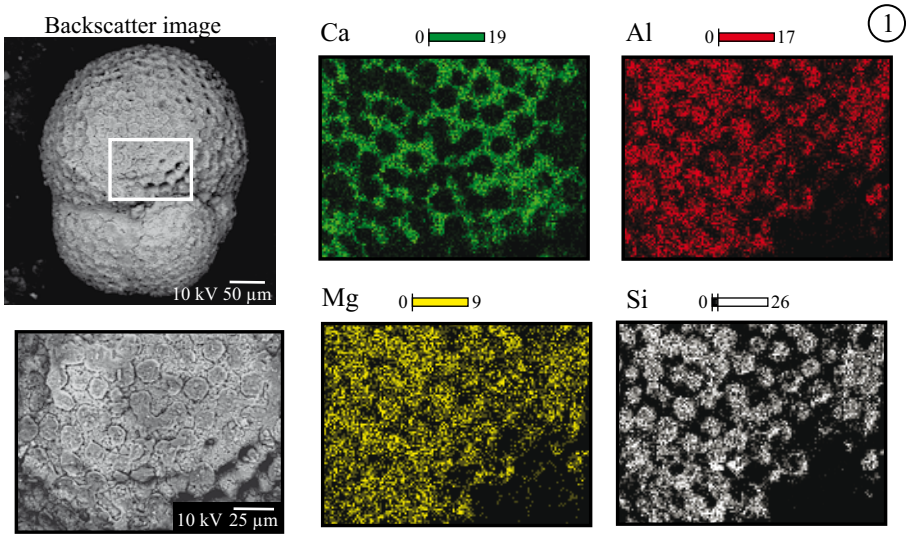

Figure 8. EDS mapping of an individual presenting oxidized coating. 1. Superficial distribution of calcium, aluminum, magnesium and silica in a *Globigerinoides trilobus* test. Calcium is restricted to the interpore areas, as aluminum, silica and magnesium are concentrated in the pores.

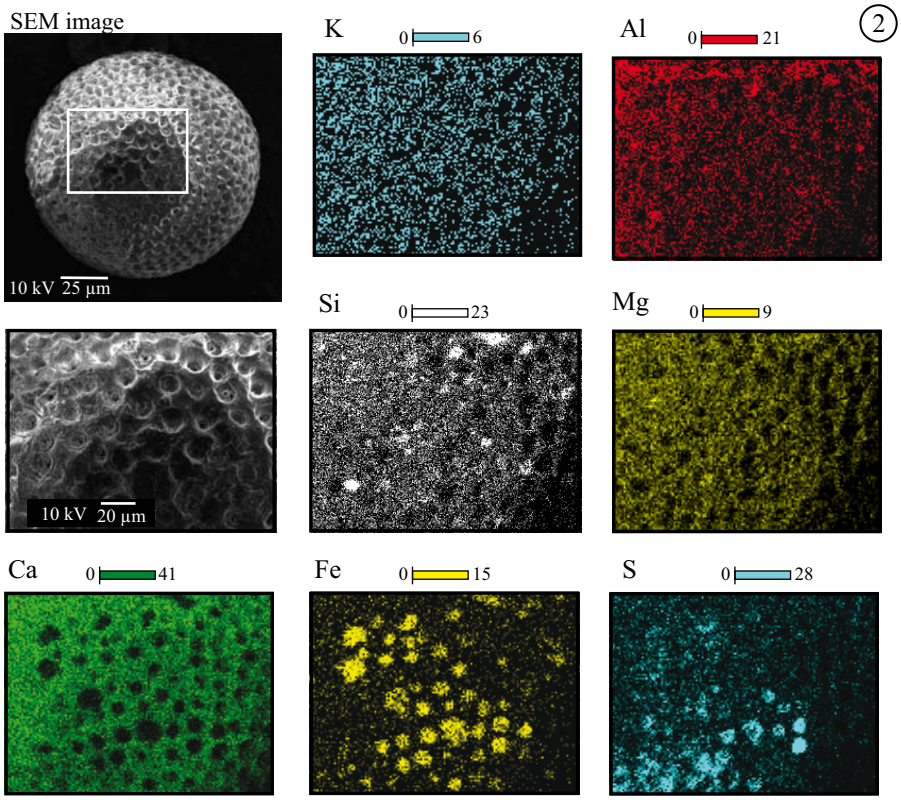

Figure 9. Distribution of potassium, aluminum, calcium, magnesium, iron and sulfur in the test surface of an *Orbulina universa* specimen. Calcium is markedly concentrated in interpore areas while the other elements are dispersed on the surface and locally concentrated in the pores. Intensity values are expressed in counts per second (cps). The accompanying SEM/backscatter images show the areas selected for elemental mapping.

Additionally, the Miocene section of the Pelotas Basin represents a record of a regressive episode, which is marked by disconformities and turbidite deposition (Fontana, 1996). Thus, these deposits are punctuated of discontinuities of regional extension as observed by Fontana (1996) and Anjos-Zerfass (2009), that may have promoted pathways to meteoric water percolation and, consequently, the oxidation of the clay mineral films.

Stable isotope data

To perform carbon and oxygen isotope analyses, well-preserved specimens from drill-holes PEL-1, PEL-2 and PEL-2A were selected to compose monogeneric samples.

Specimens of samples proceeding from wells 2-TG-96-RS and PEL-3 were not collected for isotopic analyses since all the foraminifera tests in these samples presented signs of dissolution, such as deepening of the sutures, superficial corrosion and widening of the opening, as well as calcite infill, found in some samples of the PEL-3 drill-hole. Oxygen and carbon isotope data of the foraminiferal tests are presented in Table 1.

The analyzed samples are distributed into two groups of values, one presenting clustered data of heavier compositions (F1 group) and the other with scattered data of lighter compositions (F2 group), as shown in the $\delta^{18}O$ *versus* $\delta^{13}C$ plots (Figure 10). Samples of the F1 group present $\delta^{18}O$ values similar to those observed in marine carbonates, specially the values measured in planktic foraminifera tests recovered from sediments of Late Miocene age in the ODP/DSDP sites (Hoefs, 2009; Williams *et al.*, 2005). The isotopic compositions of the F2 group tests are much lighter than the marine carbonates, with more negative values of $\delta^{18}O$ and $\delta^{13}C$ (Figure 10). This pattern of distribution of the isotopic compositions is very similar to those previously observed by Shieh *et al.* (2002) in Miocene-Pleistocene deposits of Taiwan.

Lighter isotopic compositions (F2 group) occurred in the interval where neomorphism and calcite infill occur in a pervasive form, from between 1,404 and 1,638 m in drill-hole PEL-1 and 2,898 and 3,114 m depths of drill-hole PEL-2; these coincide with the intervals where the specimens presented the highest levels of alteration of the microstructure. In these intervals, the tests presented neomorphism of the wall, and eventually, these tests had secondary calcite crystals inside their chambers (Figures 4.3a and 4.5a).

According to Schrag *et al.* (1995), the values of $\delta^{18}O$ usually decline with increases in burial depth. However, in the studied drill-holes, the $\delta^{18}O$ values oscillate between -1.42 ‰ and 0.57 ‰ in drill-hole PEL-1 and between

Table 1. Oxygen and carbon isotope composition of Planktonic foraminifera shells from Miocene deposits of Pelotas Basin.

Drill-hole	Sample (m)	$\delta^{18}O$ (PDB)	$\delta^{13}C$ (PDB)	Species	Drill-hole	Sample	$\delta^{18}O$ (PDB)	$\delta^{13}C$ (PDB)	Species
PEL-1	1,044	-0.50	2.27	*O. universa*	PEL-2	2,268	-0.47	2.65	*Gs. immaturus*
PEL-1	1,116	0.57	1.53	*G. venezuelana*	PEL-2	2,304	0.62	2.19	*Globorotalia* sp.
PEL-1	1,134	-0.18	1.92	*O. universa*	PEL-2	2,340	3.54	0.04	*Globigerina* sp.
PEL-1	1,152	-1.42	2.40	*Gs. trilobus immaturus*	PEL-2	2,340	-0.48	2.50	*O. universa*
PEL-1	1,152	-0.81	1.45	*O. universa*	PEL-2	2,376	0.71	1.79	*Globorotalia* sp.
PEL-1	1,170	-0.47	2.23	*O. universa*	PEL-2	2,412	0.66	1.38	*Globorotalia* sp.
PEL-1	1,188	0.53	1.59	*Gr. miozea/conomiozea*	PEL-2	2,448	-0.01	1.00	*G. venezuelana*
PEL-1	1,206	-0.74	2.31	*Gs. trilobus sacculifer*	PEL-2	2,466	0.77	1.75	*Globigerina* sp.
PEL-1	1,224	0.58	1.28	*Gr. miozea/conomiozea*	PEL-2	2,484	0.40	1.45	*Gq. dehicens*
PEL-1	1,260	-0.91	3.11	*O. universa*	PEL-2	2,592	-0.24	2.88	*O. universa*
PEL-1	1,278	0.23	1.30	*Gr. miozea/conomiozea*	PEL-2	2,628	0.67	1.92	*Globorotalia* sp.
PEL-1	1,296	0.12	1.43	*Gr. miozea/conomiozea*	PEL-2	2,628	-0.33	2.22	*O. universa*
PEL-1	1,314	-0.09	1.23	*Gr. miozea/conomiozea*	PEL-2	2,664	-0.13	2.23	*O. universa*
PEL-1	1,314	-0.97	1.92	*O. universa*	PEL-2	2,700	-0.50	2.58	*O. universa*
PEL-1	1,332	-0.01	2.34	*O. universa*	PEL-2	2,700	0.24	1.53	*Globorotalia* sp.
PEL-1	1,332	0.28	1.63	*Gr. miozea/conomiozea*	PEL-2	2,736	-0.38	1.82	*O. universa*
PEL-1	1,350	0.53	1.01	*Globorotalia sp.*	PEL-2	2,808	0.48	1.61	*G. venezuelana*
PEL-1	1,350	-0.92	1.70	*O. universa*	PEL-2	2,862	-0.89	1.62	*O. universa*
PEL-1	1,386	0.40	1.21	*O. universa*	PEL-2	2,862	0.33	1.77	*Globorotalia* sp.
PEL-1	1,404	-3.13	-0.38	*Gs. trilobus immaturus*	PEL-2	2,898	0.59	1.42	*G. venenzuelana*
PEL-1	1,512	-3.37	0.09	*Gs. trilobus immaturus*	PEL-2	2,962	-3.92	-3.60	*O. universa*
PEL-1	1,548	-3.55	0.16	*Gs. trilobus immaturus*	PEL-2	3,114	-3.34	0.03	*Globigerina* sp.
PEL-1	1,566	-5.66	0.54	*O. universa*	PEL-2	3,132	-3.94	-1.01	*G. venezuelana*
PEL-1	1,602	-2.84	-0.86	*Gs. trilobus*	PEL-2	3,132	-6.23	-2.17	*Globigerina* sp.
PEL-1	1,638	-0.41	1.89	*O. universa*	PEL-2A	1,300.8	-1.35	2.09	*Gs. trilobus trilobus*
PEL-1	1,818	0.07	1.43	*Gq dehicens*	PEL-2A	1,306.1	-1.43	2.23	*Gs. trilobus trilobus*
PEL-2	2,178	-0.01	2.36	*O. universa*					
PEL-2	2,214	0.47	1.47	*Globorotalia* sp.					

3.54‰ and 0.89‰ in drill-hole PEL-2 (Figure 11). The mimetic effect in $\delta^{13}C$ and $\delta^{18}O$ curves for depths greater than 1,400 m for PEL-1 and at depths greater than 2,862 m with relation to PEL-2 may represents an artifact produced by diagenesis, modulating both isotopic signals.

As previously verified (Sexton *et al.*, 2006; Veizer *et al.*, 1999; Scholle and Arthur, 1980), $\delta^{13}C$ is less susceptible to diagenetic alteration when compared with $\delta^{18}O$. Likewise, the isotopic data from drill-holes PEL-1 and PEL-2 show narrower ranges for the carbon data. The shift of the isotopic ratios in drill-hole PEL-1 is 3.97 ‰ for carbon and 6.94‰ for oxygen, while for drill-hole PEL-2 it is 6.48 ‰ and 9.77 ‰ for carbon and oxygen, respectively.

Neomorphism (recrystallization) during early diagenesis acts to increase the $\delta^{18}O$ values (Killingley, 1983; Williams *et al.*, 2005). Conversely, in the interval where the occurrence of neomorphism was observed, the $\delta^{18}O$ values are negative. This can indicate that this trend of lighter isotopic ratios would be related to the non-marine carbonate interaction. It is plausible that the shift of the isotopic compositions in the direction of negative values in the studied samples derive from the dissolution and re-precipitation of carbonate, since non-marine carbonates are enriched in ^{16}O and ^{12}C (Friedman, 1998).

According to Scholle and Arthur (1980), the degree of isotopic composition alterations in the pelagic carbonate depends on the level of diagenetic changes. The oxidation of the organic matter after the burial of the sediments promotes the enrichment in ^{12}C of the dissolved carbon, which can contribute to the formation of isotopically lighter cements. As a result, the secondary calcite formed inside and on the foraminifera tests of the deeper intervals in drill-hole PEL-1 could be a factor contributing to the lighter isotopic composition observed in the analyses. These crystals are exchange products of the interaction between the tests and the water with organic matter dissolved (Shieh *et al.*, 2002). This implies a strong influence on the isotopic composition, and, consequently, indicates that the data obtained from these samples should not be used for paleoenvironmental interpretation.

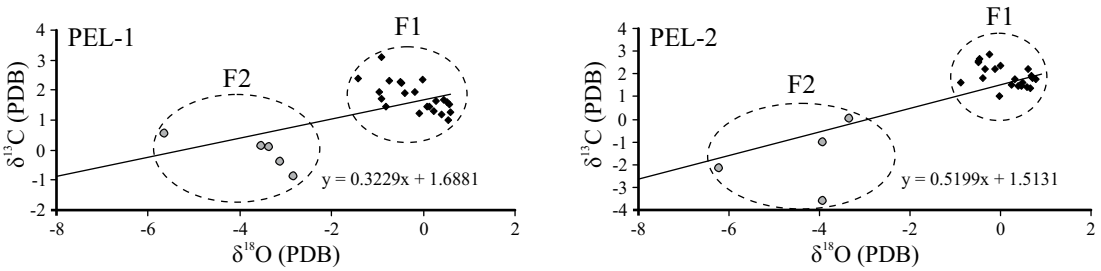

Figure 10. Plots of $\delta^{18}O$ (V-PDB) *versus* $\delta^{13}C$ (V-PDB) of 46 monogeneric samples.

CONCLUSIONS

The combination of imaging techniques and chemical/isotopic analyses allow the identification of post-depositional alterations in foraminifera tests. On this basis, it is possible to select adequate material with which to attain isotopic data aimed at paleoenvironmental characterization. To perform this study, two species were chosen (*Orbulina universa* and *Globigerinoides trilobus*). The selected specimens were investigated using scanning electron microscopy (SEM), energy dispersive spectrometry (EDS) and stable isotope analyses.

By means of SEM imaging, it was possible to identify the alterations of the original wall texture features as dissolution, neomorphism (recrystallization) and coating of autigenic minerals. The application of the EDS technique allowed us to recognize the distribution of Ca, Mg, Al, Si, Fe and S with the texturally well-preserved tests presenting unaltered calcitic composition, whereas those with textural alterations exhibited variable contributions of Mg, Si, Al, Fe and S.

The stable isotopic data indicated the degree of alteration, thus defining two major groups (F1 and F2). The heavier values and narrower range of the $\delta^{18}O$ and $\delta^{13}C$ of the F1 group (-6.23 to -2.84 and -3.60 to 0.54, respectively) suggest that the environmental signal could be preserved in this isotopic record; however, the lighter and scattered values of the F2 group (-1.42 to -3.54 and 0.04 to 3.11, respectively) indicate a signal derived from post-depositional alterations, and, consequently, the data obtained from these samples should not be used in paleoenvironmental interpretations.

The application of these combined techniques in Miocene foraminifera from the Pelotas basin unequivocally indicate the material suitable for providing accurate paleoenvironmental information, as in many cases the alterations carried out by diagenesis are detected only by means of the analyses of textural patterns at the micrometric scale and/or isotopic analyses.

ACKNOWLEDGEMENTS

The authors gratefully acknowledge Petrobras (Petróleo Brasileiro S.A.) and CPRM (Geological Survey of Brazil) for providing the drill-hole samples. We are indebted to Victor Pereira (UFRGS) for his suggestions and to Francisco Vega (UNAM) for the linguistic revision. The authors are very grateful to Alcides Nobrega Sial and Valesca Maria Portilla Eilert who reviewed the manuscript and made helpful comments and suggestions. G. S. Anjos-Zerfass thanks the Brazilian National Petroleum Agency (ANP) for the grant.

REFERENCES

Adelseck, C.G. Jr., 1978, Dissolution of deep-sea carbonate: preliminary calibration and morphological aspects: Deep-sea Resource, 24, 1167-1185.

Anjos-Zerfass, G.S., 2009, Estudos paleoambientais com base em isótopos de carbono, oxigênio e estrôncio em foraminíferos do Terciário

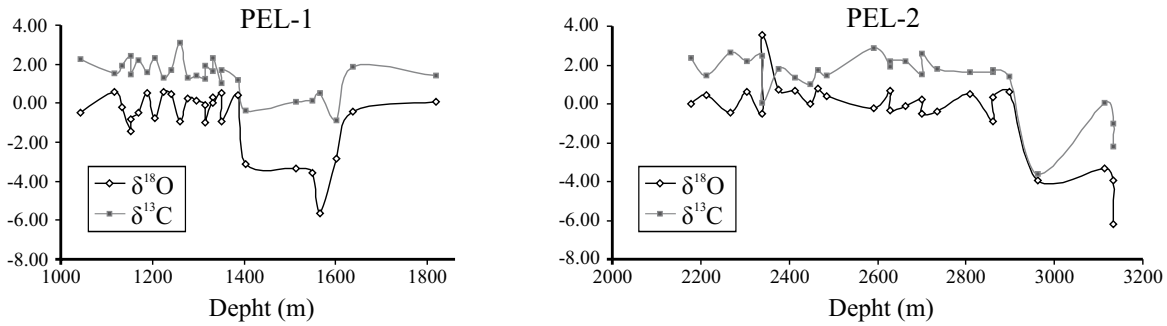

Figure 11. Plots of $\delta^{18}O$ and $\delta^{13}C$ *versus* depth for drill-holes PEL-1 and PEL-2.

da Bacia de Pelotas: Porto Alegre, Brasil, Universidade Federal do Rio Grande do Sul, Tesis doctoral, 233 pp.

Bemis, B.E., Spero, H.J., Bijma, J., 1998, Reevaluation of the oxygen isotopic composition of planktic foraminifera: Experimental results and revised temperature equations: Paleoceanography, 13(2), 150-160.

Bemis, B.E., Spero, H.J., Lea, D.W., Bijma, J., 2000, Temperature influnce on the carbon isotopic composition of *Globigerina bulloides* and *Orbulina universa* (planktonic foraminifera): Marine Micropaleontology, 38, 213-228.

Berner, R.A., 1981, A new geochemical classification of sedimentary environments: Journal of Sedimentary Petrology, 51(2), 359-365.

Berner, A., 1984, Sedimentary pyrite formation: an update: Geochimica et Cosmochimica Acta, 48(4), 605-615.

Bolli, H.M., Saunders, J.B., 1985, Oligocene to Holocene low latitude planktic foraminifera, *in* Saunders, J.B., Perch-Nielsen, K. (eds.), Plankton Stratigraphy: Cambridge, Cambridge University Press, 155-262.

Brown, S.J., Elderfield, H., 1996, Variations in the Mg/Ca and Sr/Ca ratios of planktonic foraminifera caused by postdepositional dissolution: Evidence of shallow Mg-dependent dissolution: Paleoceanography, 11(5), 543-551.

Budd, D.A., Hiatt, E.E., 1993, Mineralogical stabilization of high-magnesium calcite: geochemical evidence for intercrystal recrystallization within porcelaneous foraminifera: Journal of Sedimentary Petrology, 63(2), 261-274.

Bueno, G.V., Zacharias, A.A., Oeiro, S.G., Cupertino, J.A.; Falkenhein, F.U.H., Martins Neto, M.A., 2007, Bacia de Pelotas: Boletim de Geociências da Petrobras, 15(2), 551-559.

Collen, J.D., Burgess, C.J., 1979, Calcite dissolution, overgrowth and recrystallization in the benthic foraminiferal genus *Notorotalia*: Journal of Paleontology, 53(6),1343-1353.

Chemale Jr., Costa, K. B., Soliani Jr., E., Kawashita, K., Castro, G., Rodrigues, R., Azevedo, R. L., Johnson, C., Lauca, E., 2002, Estratigrafia química do Cenozóico da margem continental brasileira: Relatório 01/LGI-UFRGS, 41 pp.

Closs, D., 1970, Estratigrafia da Bacia de Pelotas, Rio Grande do Sul: Iheringia (Série Geologia), 3, 3-37.

Dias, J.L., Silveira, D.P., Sad, A.R.E., Latgé, M.A.L., 1994, Bacia de Pelotas: Estágio atual do conhecimento geológico: Boletim de Geociências da Petrobras, 8(1), 235-245.

Faure, G., 1986, Principles of isotope geology: New York, John Willey, 345 pp.

Fontana, R,L., 1996, Geotectônica e sismoestratigrafia da Bacia de Pelotas e Plataforma de Florianópolis Porto Alegre, Brasil: Universidade Federal do Rio Grande do Sul, Tesis doctoral, 214 pp.

Friedman, G.M., 1998, Temperature and salinity effects on ^{18}O fractionation for rapidly precipitated carbonates. Laboratory experiments with alkaline lake water – Perspective: Episodes, 21, 97-98.

Hecht, A.D., Eslinger, E.V., Garmon, L.B., L.B., 1975, Experimental studies on the dissolution of planktonic foraminifera: Cushman Foundation for Foraminiferal Research, Special Publication 13, 56-69.

Hoefs, J., 2009, Stable isotope geochemistry: Berlin, Springer-Verlag, 340 pp.

Kennett, J.P., Srinivasan, S., 1983, Neogene planktonic foraminifera: Stroudsburg, Hutchinson Ross Publishing Company, 265 pp.

Killingley, J.S., 1983, Effects of diagenetic recrystallization on $^{18}O/^{16}O$ values of deep-sea sediments: Nature, 301, 594-597.

Kowsmann, R.O., Francisconi, O., Leyden, R., 1974, Refração sísmica marinha nas bacias de Pelotas, Santos Sul e na Plataforma de Torres, *in* Congresso Brasileiro de Geologia, 28, Porto Alegre: Brasil, Sociedade Brasileira de Geologia, Anais, 3, 283-295.

Lohmann, G. P., 1995, A Model for variation in the chemistry of planktonic foraminifera due to secondary calcification and selective dissolution: Paleoceanography, 10(3), 445-457.

McArthur, J.M., 1994, Recent trends in strontium isotope stratigraphy: Terra Nova, 6, 331-358.

Morad, S., Ketzer, J.M., De Ros, L.F., 2000, Spatial and temporal distribution of diagenetic alterations in siliciclastics rocks: implications for mass transfer in sedimentary basins: Sedimentology, 47, 95-120.

Odin, G.S., Fullagar, P.D., 1988, Geological significance of the glaucony facies, *in* Odin, G.S. (ed.), Green Marine Clays: Amsterdam, Elsevier, Developments in Sedimentology, 45, 295-232.

Rosa, A.P., 2007, Interpretação sismo-estratigráfica da porção da Bacia de Pelotas que engloba o Cone do Rio Grande e a avaliação do seu potencial petrolífero: Macaé, Brazil, Universidade Estadual do Norte Fluminense, Laboratório de Engenharia e Exploração de Petróleo, Tesis doctoral, 283 pp.

Sadekov, A. Y., Eggins, S.M., Klinkhammer, G.P., Rosenthal, Y., 2010. Effects of seafloor and laboratory dissolution on the Mg/Ca compositon of *Globigerinoides sacculifer* and *Orbulina universa* tests: A laser ablation ICPMS microanalysis perspective: Earth and Planetary Science Letters, 292(3-4), 312-324.

Sanyal, A., Bijma, J., Spero, H. J.; Lea, D. W., 2001, Empirical relationship between pH and the boron isotopic composition of *Globigerinoides sacculifer*: Implications for the boron isotope paleo-pH proxy: Paleoceanography, 16, 515–519.

Savin, S.M., Douglas, R.G., 1973, Stable isotope and magnesium geochemistry of recent planktonic foraminifera from South Pacific: Geological Society of America Bulletin, 84(7), 2327-2342.

Scholle, P. A., Arthur, M.A., 1980, Carbon isotope fluctuations in cretaceous pelagic limestones: potential stratigraphic and petroleum exploration tool: American Association of Petroleum Geologists Bulletin, 64(1), 67-87.

Schrag, D. P., DePaolo, D.J., Richter, F.M., 1995, Reconstructing past sea surface temperatures: Correcting for diagenesis of bulk marine carbonate: Geochimica et Cosmochimica Acta, 59(11), 2265-2278.

Sexton, P.F.; Wilson, P.A., Pearson, P.N., 2006, Microstructural and geochemical perspectives on planktonic foraminiferal preservation: "glassy" *versus* "frosty": Geochemistry, Geophysics, Geosystems 7(Q12P19).

Shieh, Y.-T., You, C.-F., Shea, K.-S, Horng, C.-S., 2002, Identification of artifacts in foraminiferal tests using carbon and oxygen isotopes: Journal of Asian Earth Sciences, 21, 1-5.

Siesser, W.G., Rogers, J., 2006, Authigenic pyrite and gypsum in South West African continental slope sediments: Sedimentology, 23(4), 567-577.

Spero, H. J., Lea, D.W., 1993, Intraspecific stable isotope variability in the planktic foraminifera *Globigerinoides sacculifer*: Results from laboratory experiments: Marine Micropaleontology, 22, 221-234.

Stainforth, R.M., Lamb, J.L., Luterbacher, H.; Beard, J.H., Jeffords, R.M., 1975, Cenozoic planktonic foraminiferal zonation and characteristics of index forms: Lawrence, The University of Kansas, Paleontological Contributions, 62, 425 pp.

Veizer, J., Ala, D.; Azmy, K., Brucschen, P., Bruhn, F., Carden, G.A.F., Diener, A., Ebneth, S., Godderis, Y., Jasper, T., Korte, C., Pawllek, F., Podlaha, O.G., Strauss, H., 1999, $^{87}Sr/^{86}Sr$, $\delta^{13}C$ and $\delta^{18}O$, evolution of Phanerozoic seawater: Chemical Geology, 161, 59-88.

Williams, M., Haywood, A.M., Taylor, S.P., Valdes, P.J., Sallwood, B.W., Hillenbrand, C.-D., 2005, Evaluating the efficacy of planktonic foraminifer calcite $\delta^{18}O$ data for sea surface temperature reconstruction for the Late Miocene: Geobios, 38, 843-863.

Williams, M., Haywood, A.M., Vautravers, M., Sellwood, B.W., Hillenbrand, C.-D., Wilkinson, I.P.A., Miller, C.G., 2007, Relative effect of taphonomy on calcification temperature estimates from fossil planktonic foraminifera: Geobios, 40, 861-874.

Zeebe, R.E., Bijma, J. Sanyal, A.; Spero, H., Wolf-Gladrow, D.A., 2008, Vital effects and beyond: A modelling perspective on developing paleoceanographical proxy relationships in foraminifera: Geological Society of London Special Publication, 303, 45-58.

Manuscript received: June 9, 2010
Corrected manuscript received: September 23, 2010
Manuscript accepted: October 2, 2010